



01 Jan 1997

Prediction of Yarn Strength from Fiber Properties Using Fuzzy ARTMAP

Raonak Zaman

Donald C. Wunsch

Missouri University of Science and Technology, dwunsch@mst.edu

Follow this and additional works at: https://scholarsmine.mst.edu/ele_comeng_facwork

 Part of the [Electrical and Computer Engineering Commons](#)

Recommended Citation

R. Zaman and D. C. Wunsch, "Prediction of Yarn Strength from Fiber Properties Using Fuzzy ARTMAP," *Proceedings of the International Conference on Vision, Recognition, Action: Neural Models of Mind and Machine*, Boston University, Jan 1997.

This Article - Conference proceedings is brought to you for free and open access by Scholars' Mine. It has been accepted for inclusion in Electrical and Computer Engineering Faculty Research & Creative Works by an authorized administrator of Scholars' Mine. This work is protected by U. S. Copyright Law. Unauthorized use including reproduction for redistribution requires the permission of the copyright holder. For more information, please contact scholarsmine@mst.edu.

Prediction of Yarn Strength from Fiber Properties using Fuzzy ARTMAP

Raonak Zaman Raonak@ttu.edu
Donald C. Wunsch Dwunsch@coe2.coe.ttu.edu

Applied Computational Intelligence Laboratory
Electrical Engineering
Texas Tech University
Box 43012, Lubbock, TX 79409-3102
Internet: <http://www.acil.ttu.edu>

ABSTRACT

The count-strength-product (CSP) of cotton yarn is a complex function of fiber properties and spinning performance. The traditional way of predicting yarn CSP is using linear multiple regression. The correlation coefficient between actual CSP and predicted CSP obtained from linear regression is almost always less than 0.9. In this paper, we used a Fuzzy ARTMAP network to predict yarn CSP from fiber properties and spinning performance. Fiber properties and spinning data were used as inputs to ART_a , and yarn CSP was used as ART_b input. Our objectives are: better prediction of the quality of the end product, and to determine the optimum set of fiber properties to make reliable predictions. Several experiments were designed with different combinations of fiber properties (based on the measuring instruments used in collecting those properties) as ART_a inputs. To improve relative accuracy of prediction, three voter networks were used in each experiment. During training, order of the training data was scrambled to create 3 ARTMAP networks. The ART_b templates in the voter networks indicates the range of CSP for any particular inputs to the ART_a . Since CSP is a continuous analog value, the boundary of ART_b templates is usually not fixed among the voters. To improve absolute accuracy of prediction, we took a Fuzzy OR function among the three chosen voter templates during recall to reduce the span of the range. When predicting, each ART_b template is represented by its center of gravity. In each experiment, the correlation coefficient between the actual and the predicted CSP was better than 0.95. A combination of all fiber properties from traditional and Advanced Fiber Information System (AFIS) tests made marginally better prediction than any other combination of fiber properties including when fiber properties from all the tests were fed into ART_a .

Introduction

The prerequisite for success of cotton textile manufacturers in today's global market is reliable, cost-effective quality control. The primary mechanism for achieving this is (a) appropriate blending of cotton and (b) proper setting of textile machinery both being based on measurements of critical fiber properties. The prerequisite for improved cotton fiber selection and blending is development of models that more accurately predicts processing efficiency and yarn quality based on objective fiber properties. Achieving this will require development of an adequate database and application of sophisticated estimation and prediction methodologies. Yarn properties depend on fiber quality and spinning performance. Usual method of predicting yarn qualities, e.g., count-strength-product, tenacity, elongation etc. is linear regression analysis. One of the drawbacks in statistical prediction is that the model, generally a linear model, should be predefined. Ethridge et. al. showed that prediction could be improved with a nonlinear model [1]; they included few quadratic and logarithmic functions of fiber properties in their model. Neural networks could be used to predict a relationship between yarn quality and fiber properties in the absence of prior knowledge of the mathematical model.

In this experiment, we used Fuzzy ARTMAP as the prediction machine. When the size of the training set is small with respect to the dimension of input vector, Fuzzy ARTMAP prediction function is more reliable than a multi-layer perceptron using back-propagation algorithm [2, 3]. Besides it provides

valuable insight of the pattern from template output. All independent variables in the experiment can be a potential input to the prediction machine. The independent variables include fiber properties, spinning data (e.g., yarn count, spin process), and cotton type (upland or ELS). The only dependent variable would be count-strength-product of the yarn. Fiber properties of each sample was measured using traditional method and the fineness/maturity measurements from the Shirley F/MT (8 properties), HVI or the Spinlab High Volume Instrument (8 properties), short fiber measurements from AFIS or the Uster Advanced Fiber Information System (5 properties). Another aspect of this project is to determine the optimum collection of fiber properties to make reliable quality prediction. Elimination of any fiber property measurement would save both time and money, in terms of equipment cost.

To make this paper self sustained we included full description of Fuzzy ARTMAP learning in Section II. Section III discusses the experiments and results.

Section II

Operation of Fuzzy ARTMAP

Fuzzy ARTMAP is a supervised clustering algorithm that operates on vectors with analog or binary valued elements. In a Fuzzy ARTMAP, categories formed by two Fuzzy ART units ART_a and ART_b , are associated via a MAP field as category and class respectively. During training, like supervised learning, independent variables are fed to the inputs of ART_a (input training signal) and dependent variables to the ART_b input (output training signal). In the recall phase, inputs are supplied only to the ART_a , and the template chosen at ART_b will serve as the predicted output. Function of the MAP field in between them is to ensure maximum code compression at ART_a templates for minimum predictive error at ART_b templates. This is done by a method called "match-tracking."

Summary of Fuzzy ART: Individually, both the ART_a and ART_b units works as Fuzzy ART units.

Each Fuzzy ART unit has three layers of nodes called F_0 , F_1 and F_2 layers respectively. Inputs to Fuzzy ART unit are in the complement code form to reduce a phenomenon called category proliferation [4]. If the input layer F_0 has M nodes (i.e., input vector is M -dimensional), then F_1 layer will have $2M$ nodes. For N output nodes at F_2 layer there will be $N \times 2M$ top down weight vector \mathbf{w}_j , connecting each F_2 layer node with F_1 layer. \mathbf{w}_j is also known as the long-term-memory (LTM) trace or templates. Fuzzy ART dynamics are determined by a choice parameter >0 ; a learning rate parameter $[0, 1]$; and a vigilance parameter $[0, 1]$.

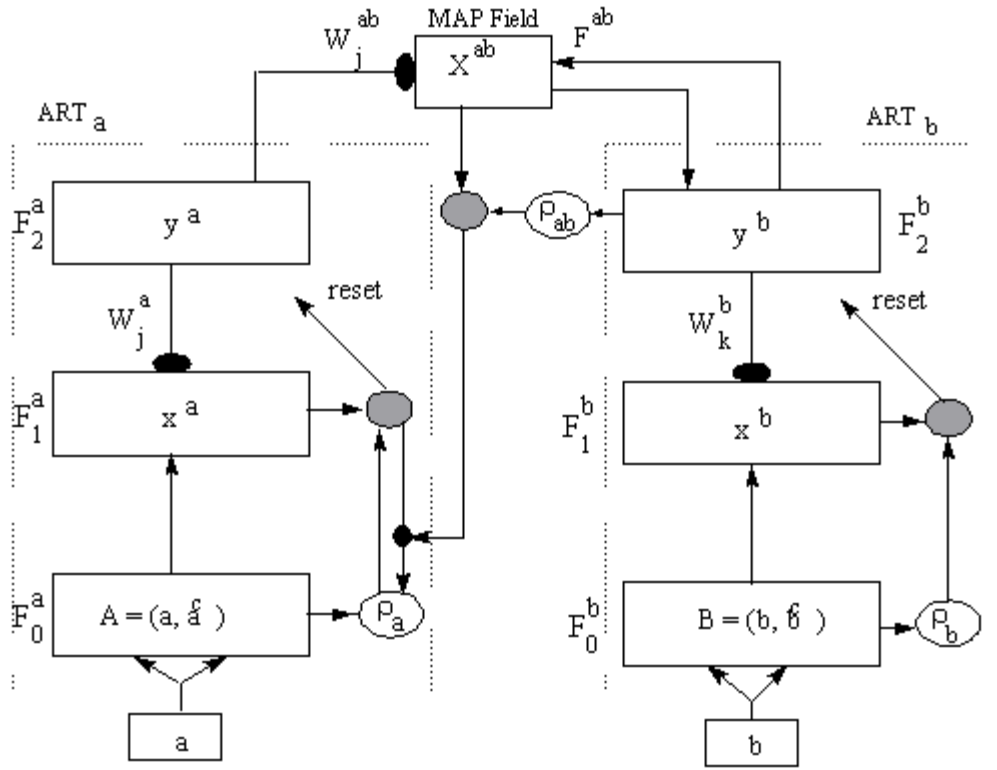


Figure 1: Architecture of Fuzzy ARTMAP [2].

Following notations will be used throughout the material regarding Fuzzy ART inputs and outputs at each layer.

1. M-dimensional input to F_0 layer, $\mathbf{A} = [\mathbf{a}]$; \mathbf{A} is normalized, i.e., a_i is $[0, 1]$.
2. 2M-dimensional output of F_0 layer, $\mathbf{I} = (\mathbf{a}, \mathbf{a}^c) =$ input to F_1 layer;

where, $\mathbf{a}^c =$ complement of \mathbf{a} , i.e., $a_i^c \equiv 1 - a_i$.

1. Output of F_1 layer is $\mathbf{x} = (x_1, x_2, \dots, x_{2M})$, where,

$$x_j = \begin{cases} I & \text{if } F_2 \text{ is inactive} \\ I \wedge w_j & \text{if the } j\text{th } F_2 \text{ node is active} \end{cases} \quad (1)$$

\mathbf{x} serves as the system output in recall phase.

1. Input to F_2 layer is given by choice function $T_j(\mathbf{I})$. For each input \mathbf{I} and F_2 node j , the choice function T_j is defined by

$$T_j(\mathbf{I}) = \frac{|I \wedge w_j|}{\alpha + |w_j|}, \quad (2)$$

where the fuzzy AND, or intersection operator $()$ is defined by:

$$(\mathbf{p} \mathbf{q})_i = \min(p_i, q_i) \quad (3)$$

and where the norm $\|\cdot\|$ is defined by:

$$\|\mathbf{p}\| = \sum_{i=1}^M p_i \quad (4)$$

for any M-dimensional vectors \mathbf{p} and \mathbf{q} . For notational simplicity, $T_j(\mathbf{I})$ is

written as T_j when the input \mathbf{I} is fixed.

1. Output of F_2 layer is $\mathbf{y} = (y_1, y_2, \dots, y_N)$. When Jth category is chosen,

$y_J = 1$; and $y_j = 0$ for $j \neq J$.

The system is said to make a category choice when at most one F_2 node can become active at a given time. The category choice is indexed by J, where, $T_J = \max\{T_j; j = 1, \dots, N\}$. If more than one T_j is maximal, the category j with the smallest index is chosen. In particular node becomes committed in the order $j=1, 2, 3$, etc. this rule eliminates the need for any bottom-up weights between F_1 and F_2 layers (some authors prefer to use them [5]).

In the training phase, the system learns by resonance and mismatch. F_1 layer output \mathbf{x} represents a compressed coding of input \mathbf{I} , and vigilance parameter determines the minimum confidence between \mathbf{x} and \mathbf{I} to accept the coding. The system is said to be in resonance if the match function $\|\mathbf{x}\| / \|\mathbf{I}\|$ of the chosen category meets the vigilance criterion:

$$\frac{\|\mathbf{x}\|}{\|\mathbf{I}\|} = \frac{\|\mathbf{I} \wedge \mathbf{w}_j\|}{\|\mathbf{I}\|} \geq \rho \quad (5)$$

Template \mathbf{w}_j then incorporate the pattern according to learning rule. Mismatch reset occurs if

$$\frac{\|\mathbf{I} \wedge \mathbf{w}_j\|}{\|\mathbf{I}\|} < \rho$$

The value of the choice function T_J is set to zero for the duration of the input presentation to prevent the persistent selection of the same category during search. A new index J is then chosen by T_j . The search process continues until the chosen j satisfies vigilance criterion. An F_2 node is said to become committed when it is being selected by any input pattern for the first time.

The Fuzzy ART top-down weights follow outstar learning [2]. Learning by \mathbf{w}_j is gated by \mathbf{y} . When a category J is chosen (\mathbf{w}_j at resonance with \mathbf{I}), weights w_{ji} change via learning rule. Templates associated with other nodes $j \neq J$ remain unchanged. The weight vector \mathbf{w}_j is updated according to the equation

$$\mathbf{w}_j^{(new)} = \rho \mathbf{I} \wedge \mathbf{w}_j^{(old)} + (1 - \rho) \mathbf{w}_j^{(old)} \quad (6)$$

Initially, $w_{ji}(0) = 1.0$, for all j and i. Templates corresponding to an uncommitted node is the same as

initial weight. Each LTM trace w_{ji} is monotonically nonincreasing through time and hence converges to a limit.

Fast learning corresponds to setting $\alpha = 1.0$. During fast learning, adaptive weights reach their asymptote on each input representation. If $0 < \alpha < 1$ it is called slow learning. A special type of slow learning, called fast-commit slow-encode, is one in which fast learning occurs when the chosen F_2 node is uncommitted, and slow learning occurs when it is committed.

Geometric interpretation of Fuzzy ART: In fast learn scenario, a committed template w_J , which has coded input patterns $I_1 = (a(1), a^c(1)), I_2 = (a(2), a^c(2)), \dots, I_P = (a(P), a^c(P))$, can be written as :

$$w_J = I_1 \wedge I_2 \wedge \dots \wedge I_P = \left(\bigwedge_{i=1}^P a(i), \bigwedge_{i=1}^P a^c(i) \right) = \left(\bigwedge_{i=1}^P a(i), \left\{ \bigvee_{i=1}^P a(i) \right\}^c \right) = (u_J, v_J)^c \quad (7)$$

Thus, the weight vector w_J , can be represented, geometrically, in terms of two points, u_J , and v_J , in the M -dimensional space. Also, it can be represented geometrically as a hyper-rectangle with endpoints u_J , and v_J . With the same reasoning, any input vector $I = (a, a^c)$ is equivalent to a point in the hyper-space. When a template becomes committed for the first time, it is a point in space or a hyper-rectangle of size zero. As more and more inputs are coded into the template the size of the hyper-rectangle gets bigger and bigger. Note that, the size of the hyper-rectangle with endpoints u_J , and v_J is taken to be equal to $|v_J - u_J|$ [2, 6].

$$\text{Now, } |w_J| = \sum_i (u_J)_i + \sum_i [1 - (v_J)_i] = M - |v_J - u_J|$$

i.e., the size of the hyper-rectangle R_j is :

$$|R_j| = M - |w_j|$$

But, for vigilance criteria, $|w_j| \geq \rho M$. Thus,

$$|R_j| \leq (1 - \rho)M$$

When $|R_j| \rightarrow 0$, the template represents rare inputs or outliers. As $|R_j|$ gets bigger than zero or $|w_j|$ gets smaller than M , more and more input points are mapped inside the hyper-rectangle. This second situation represents generalization among input patterns.

Effect of alpha: To explain the effect of choice factor α , let us write the equation of choice function one more time.

$$T_j(I) = \frac{|I \wedge w_j|}{\alpha + |w_j|} \quad (2)$$

From the above equation it is clear that if $\alpha \gg |w_j|$, T_j is proportional to $|I \wedge w_j|$ only; and T_j can pick uncommitted node over committed nodes. So, initially a safe limit would be to keep $\alpha < M$.

Now, any committed weight template can be described as a subset template, mixed template or superset

template of an input I . In a subset template, $w_{ji} \leq I_i$ for all i ; i.e., $|I \wedge w_j| = |w_j|$. On the other hand, in a superset template, $w_{ji} \geq I_i$ for all i ; or, $|I \wedge w_j| = |I_j| \leq |w_j|$. For a mixed template, $|I \wedge w_j|$ is less than both $|w_j|$ and $|I_j|$. Due to the complement coding nature of the input patterns, superset templates cannot be created in a Fuzzy ART architecture with fast learning or fast-commit slow-recode learning; all superset templates are uncommitted templates.

When α is very small ($\alpha \rightarrow 0$), choice function is biased to select a subset template, because T_j is very close to 1 for a subset template. But to prevent selecting a mixed node over a subset node α has to be still smaller than some threshold value. Let w_1 be a subset node and w_2 be a mixed node of input pattern I . To choose w_1 before w_2 :

$$\frac{|w_1|}{\alpha + |w_1|} > \frac{|w_2 \wedge I|}{\alpha + |w_2|}$$

$$\text{or, } \alpha < \frac{|w_1|(|w_2| - |w_2 \wedge I|)}{|w_2 \wedge I| - |w_1|}$$

To find a maximum limit for α :

$$\max\{|w_2 \wedge I|\} M,$$

$$\min\{|w_1|\} M;$$

$$\text{therefore, } \alpha_{\max} < \frac{\rho(|w_2| - |w_2 \wedge I|)}{1 - \rho}$$

For binary input patterns $(|w_2| - |w_2 \wedge I|) = 1$. But for analog patterns it can be extremely small depending on the scaling of the input vector. For $\rho = 0.5$ and $(|w_2| - |w_2 \wedge I|) = 0.001$ (corresponding to a maximum scale factor of 1000), α has to be smaller than 0.001 to prevent choosing a mixed node before any subset node. Biasing towards selecting a subset node first would ensure maximum code compression; all the hyper-rectangles will try to acquire its maximum allowed area set by the vigilance parameter.

Geometrically, a subset template is one which encloses input point inside its hyper-rectangle and for mixed template the input point lies outside of the hyper-rectangle.

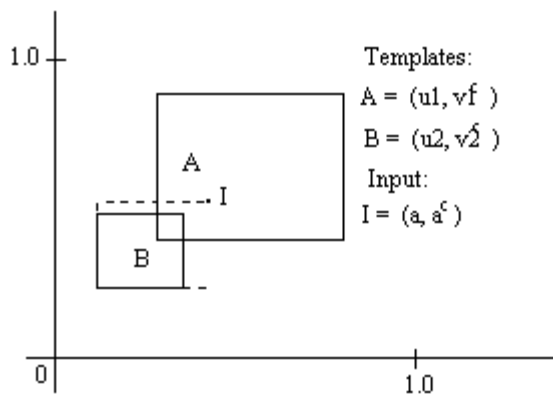


Figure 2: Geometrical representation of 2-D templates A and B. A is a subset template for I, but B is a mixed template. For 0, I will select template A first, but for B will be selected first because the new template involving B and I (dashed box) will be smaller than original template A.

Fuzzy ARTMAP summary: Let us denote ART_a input $\mathbf{I} = \mathbf{A} = (\mathbf{a}, \mathbf{a}^c)$ and ART_b input $\mathbf{I} = \mathbf{B} = (\mathbf{b}, \mathbf{b}^c)$. Variables in ART_a or ART_b are designated by superscripts a or b. For ART_a , $\mathbf{x}^a (x_1^a, \dots, x_{2M_a}^a)$ denotes the F_1^a output vector; $\mathbf{y}^a (y_1^a, \dots, y_{N_a}^a)$ denotes the F_2^a output vector; and $\mathbf{w}_j^a = (w_{j,1}^a, w_{j,2}^a, \dots, w_{j,2M_a}^a)$ denotes the j th ART_a weight vector. For ART_b , $\mathbf{x}^b (x_1^b, \dots, x_{2M_b}^b)$ denotes the F_1^b output vector; $\mathbf{y}^b (y_1^b, \dots, y_{N_b}^b)$ denotes the F_2^b output vector; and $\mathbf{w}_k^b = (w_{k,1}^b, w_{k,2}^b, \dots, w_{k,2M_b}^b)$ denotes the k th ART_b weight vector. ART_a and ART_b are linked via an inter-ART module, F^{ab} , called a map field. For the map field, $\mathbf{x}^{ab} (x_1^{ab}, \dots, x_{N_b}^{ab})$ denotes the F^{ab} output vector and $\mathbf{w}_j^{ab} = (w_{j,1}^{ab}, w_{j,2}^{ab}, \dots, w_{j,N_b}^{ab})$ denotes the weight vector from the j th F_2^a node to F^{ab} . Components of vectors \mathbf{x}^a , \mathbf{x}^b , and \mathbf{x}^{ab} are reset to zero between input presentations. Initially, each weight is set equal to one. Note, that $|A| = M_a$ and $|B| = M_b$ for all input vectors \mathbf{a} and \mathbf{b} for complement coding.

Map field activation: Map field F^{ab} is activated when one of the ART_a or ART_b categories become active. When the J th F_2^a node is chosen, F_2^a F^{ab} input is proportional to the weight vector \mathbf{w}_J^{ab} . When the K th F_2^b node is chosen, the F^{ab} node K is activated by one-to-one pathways between F_2^b and F^{ab} . If both ART_a and ART_b are active, the F^{ab} activity reflects the degree to which a correct prediction has been made. With fast learning, F^{ab} remains active only if ART_a predicts the same category as ART_b , via the weight vector \mathbf{w}_J^{ab} , or if the chosen ART_a category J has not yet learned an ART_b prediction. In summary, the F^{ab} output vector \mathbf{x}^{ab} obeys

$$x^{ab} = \begin{cases} y^b \wedge w_J^{ab} & \text{if the } J\text{th } F_2^a \text{ node is active and } F_2^b \text{ is active} \\ w_J^{ab} & \text{if the } J\text{th } F_2^a \text{ node is active and } F_2^b \text{ is inactive} \\ y^b & \text{if } F_2^a \text{ is inactive and } F_2^b \text{ is active} \\ 0 & \text{if } F_2^a \text{ is inactive and } F_2^b \text{ is inactive} \end{cases} \quad (8)$$

If the prediction w_J^{ab} is disconfirmed by y^b , the mismatch event triggers an ART_a search for a new category.

Match tracking : At the start of each input presentation the ART_a vigilance parameter ρ_a equals a baseline vigilance, $\bar{\rho}_a$. The map field vigilance parameter is ρ_{ab} . Match tracking is triggered by a mismatch at the map field F^{ab} , that is, if

$$|x^a| < \rho_{ab} |y^b| = \rho_{ab} \quad (9)$$

Match tracking increases ρ_a until it is slightly larger than the ART_a match value, $|A \wedge w_J^a| |A|^{-1}$, where A is the input to F_1^a and J is the index of the active F_2^a node. After match tracking, therefore

$$|x^a| = |A \wedge w_J^a| < \rho_a |A| = \rho_a M_a$$

When this occurs, ART_a search leads either to $ARTMAP$ resonance, where a newly chosen F_2^a node J satisfies both the ART_a matching criterion

$$|x^a| = |A \wedge w_J^a| \geq \rho_a |A|$$

and the map field matching criterion

$$|x^{ab}| = |y^b \wedge w_J^{ab}| \geq \rho_{ab} |y^b| = \rho_{ab}$$

or, if no such F_2^a node exists, to shutdown of F_2^a for the remainder of the input presentation. Since, $w_{ij}^a(0) = w_{jk}^{ab}(0) = 1$ and $0 < \rho_a, \rho_{ab} < 1$, $ARTMAP$ resonance always occurs if J is an uncommitted node.

Map field learning : Weights w_{jk}^{ab} in F_2^a F^{ab} path initially satisfy $w_{jk}^{ab}(0) = 1.0$.

During resonance with the ART_a category J active, w_J^{ab} approaches the map field vector \mathbf{x}^{ab} . With fast learning, once J learns to predict an ART_b category K , the association is permanent; i.e., $w_{JK}^{ab} = 1$ and $w_{jK}^{ab} = 0$ ($k \neq K$) for all time.

For slow learning mode at the map field, the learning rule is

$$\left(w_{jk}^{ab} \right)^{new} = \begin{cases} \left(w_{jk}^{ab} \right)^{old} & \text{if } j \neq J \\ \left(1 - \lambda_{ab} \right) \left(w_{jk}^{ab} \right)^{old} + \lambda_{ab} x_k^{ab} & \text{if } j = J \end{cases} \quad (10)$$

where, the map field activity $x_k^{ab} = 1$ when k is the correct ART_b category and $x_k^{ab} = 0$ otherwise. The map field learning parameter λ_{ab} determines the rate of change of the map field weights. Small values of λ_{ab} cause the system to base its prediction on a long-term average of its estimate, while values of λ_{ab} near one allow adaptation to a rapidly changing environment.

Section III

Prediction of Yarn Properties from Fiber Properties

Fuzzy ARTMAP has been used in mapping yarn properties with clusters of fiber properties. About 180 bales of cotton fiber have been collected from all over the world. The fiber properties includes all measurements from the traditional method and Shirley F/MT, Spinlab High Volume Instrument (HVI), and Uster Advanced Fiber Information System (AFIS). All the fiber properties and the corresponding measurement techniques are listed in Table I.

Cotton fibers are also grouped as Upland and ELS cotton. Each bale of cotton were spun in yarns using different type of spinning process. Upland cottons were spun into rotor and ring. ELS cotton went through three types of spinning: card, comb and rotor.

Multiple yarn sizes were spun from each cotton bale sampled; yarn size is also included as input feature. The yarn properties used as ART-B input were count-strength product (CSP).

Experiment

There are altogether five spinning processes have been used for two type of cotton. For ELS cotton there are: i) 36 card spun, ii) 36 rotor spun, iii) 50 comb spun. And, for upland cotton, there are iv) ring spun and v) rotor spun. Fiber properties for all 5 spins are collected in one database. The database is augmented by adding variables to designate cotton type, spin process and yarn count and CSP for each sample of yarn. To normalize, each variable is divided by the probable maximum value of that property as quoted by experts [7]. The properties which measure in percentage are kept as a fraction. Normalized CSP will be used as ART_b input while other variables will be ART_a inputs (24 variables). The database is divided into training set (210 samples) and test set (98 samples) by randomly picking up patterns.

Table I

Measurement	Properties
Traditional	<ol style="list-style-type: none"> 1. stelometer 2. elongation, 3. span, 4. uniformity 5. shirley, 6. micronaire 7. F/MT maturity, 8. F/MT fineness

HVI	<ol style="list-style-type: none"> 1. Strength, 2. Elongation, 3. Length, 4. Uniformity, 5. Micronaire, 6. Reflectance, 7. Yellowness, 8. Leafgrade
AFIS	<ol style="list-style-type: none"> 1. UQL, 2. Mean length, 3. Short fibers 4. Diameter 5. Neps

To determine the effectiveness of a given fiber property measurement technique, e.g., HVI or AFIS, we performed different experiments with same ART_b input but different ART_a inputs. We broke the experiments by the type of measurements used in accumulating fiber properties. Three variables to designate cotton type, spin process and yarn count has to be kept in all experiments. The training set and test set are same for all experiments.

The description of experiments are:

1. Expt. 1 : 24 variables for ART_a , fiber properties from all three measurements.
2. Expt. 2 : 11 variables for ART_a , fiber properties from traditional test only.
3. Expt. 3 : 11 variables for ART_a , fiber properties from HVI test only.
4. Expt. 4 : 8 variables for ART_a , fiber properties from AFIS test only.
5. Expt. 5 : 16 variables for ART_a , fiber properties from traditional and AFIS.
6. Expt. 6 : 16 variables for ART_a , fiber properties from HVI and AFIS tests.
7. Expt. 7 : 19 variables for ART_a , fiber properties from traditional and HVI.

In each case, learning is continued for 100% performance on training set. With fast learning, training converged in 1-3 epochs. In all experiments we used $\bar{\sigma}_a = 0.0$, $b = 0.98$ and $a_b = 1.0$. For each experiments optimum choice parameter was determined by several trial runs on training set; they ranged from 0.1 to 0.5. We allowed selection of mixed node in some occasions. Also, we fed the ART_b input temporally after ART_a has selected a node and primed a F_2 node at ART_b . Priming limits category proliferation at ART_b , without priming it might select a different node first. Since the number of training sample is quite small, we used voting criteria to improve performance on the test set. Under each experiment we created three voter networks; they used same ARTMAP parameters but different order of training sample during learning.

Results

The ART_b template in our experiment represent a line in rectangular co-ordinate system. From eq. (7) for weight $w_J = (u_J, \{v_J\}^c)$, u_J and v_J represent minimum and maximum CSP value respectively coded by template w_J . Thus each committed template represent range of CSP value, when a input test pattern selects that template. CSP range is given by: from w_{j1} to $(1 - w_{j2})$ multiplied by CSP normalizing

factor (5000 in our experiment). When three voter network selects three different templates for same input pattern, we took Fuzzy OR (max operator) function among the templates to improve accuracy of prediction. For a given input pattern range of CSP are given by:

$$CSP_{\min} = \max(w_{J1}^1, w_{K1}^2, w_{L1}^3);$$

$$CSP_{\max} = 1 - \max(w_{J2}^1, w_{K2}^2, w_{L2}^3).$$

The interval $(CSP_{\max} - CSP_{\min})$ is more compact than any of the individual voters and predicted value of CSP can be approximated by $(CSP_{\max} + CSP_{\min})/2$.

The correlation between actual CSP and predicted CSP for the test set is tabulated for each experiment. The average error is give in unit of CSP.

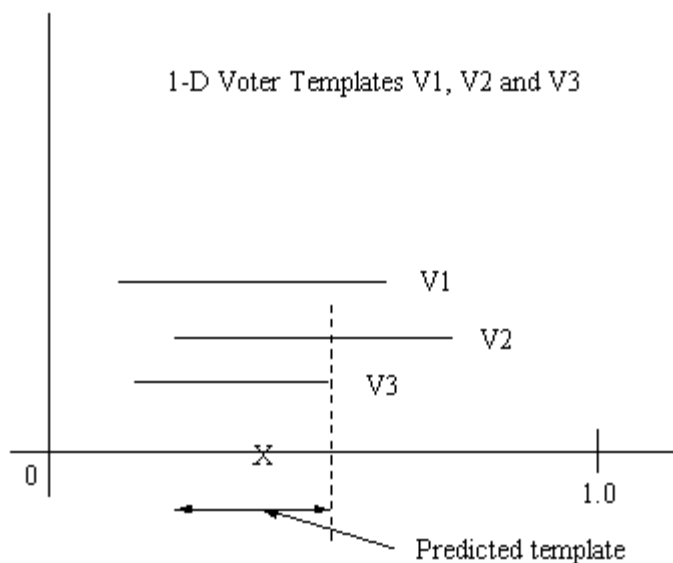


Figure 3: Improvement in accuracy is evident from ranges covered by 3 voter templates and the predicted template. Predicted template is fine enough to represent it by center of gravity marked X.

Table II

EXPT.	Input fiber properties	Correlation between actual and predicted CSP	Av. Error in CSP unit
1	All	0.9679	141.43
2	Traditional	0.9619	146.35
3	HVI	0.9662	151.53
4	AFIS	0.9567	168.24
5	Traditional & AFIS	0.9754	122.78
6	HVI & AFIS	0.9611	146.86
7	Traditional & HVI	0.9747	126.51

Conclusions

We have investigated Fuzzy ARTMAP networks for yarn strength prediction. The results show that the network provide an effective method for CSP prediction. The quality of performance is almost constant under varying input condition at ART_a, which indicates that some of the fiber properties might be linear combination of other fiber properties. It would be useful to pre-process the input data by principle component analysis to find out the independent variables. With more samples of cotton bales processed, we will make a complete comparison of statistical, Fuzzy ARTMAP and back-propagation methods for yarn property prediction in the next phase of research.

Acknowledgment

This research was supported by Advanced Technology Program.

References

1. Ethridge, M. D., Towery, J. D., and Hembree, J. F., "Estimating Functional Relationships Between Fiber Properties and the Strength of Open-End Spun Yarns," *Textile Research Journal* 52, pp. 35-45, 1982.
2. Carpenter, G., Grossberg, S. and et. al., "Fuzzy ARTMAP: A Neural Network Architecture for Incremental Supervised Learning of Analog Multidimensional Maps," *IEEE Trans. Neural Networks*, vol. 3, pp. 698-713, 1992.
3. Carpenter, G., Grossberg, S. and et., "Comparative Performance Measures of Fuzzy ARTMAP, Learned Vector Quantization, and Back Propagation for Hand Written Character Recognition," in *Proc. IJCNN-92*, vol. 1, 1992, pp. 794-799.
4. Moore B., "ART 1 and Pattern Clustering," in *Proc. of 1988 Connectionist Summer School at CMU*, pp. 174-185, San Mateo, CA: Morgan Kaufmann.
5. Georgiopoulos, M., Huang J., Heileman, G. L., "Properties of Learning in ARTMAP," *Neural Networks*, Vol. 7, no. 3, 1994, pp 495-506.
6. Georgiopoulos, M., Fernlund, H., Bebis, G., Heileman, G. L., " Order of Search in Fuzzy ART and Fuzzy ARTMAP: A Geometrical Interpretation," in *1996 ICNN Plenary, Panel and Special Sessions*, pp. 215-220, Washington D.C.
7. Personal correspondence with Reiyao Zhu, Ph.D., Head of Fiber Research, International Textile Center, Lubbock, Texas.